Deformation and Strength Criteria in Assessing Mechanical Behaviour of Joints in Historic Timber Structures

Jerzy Jasieńko[1], Marek Kardysz[2]
Prof., Wrocław University of Technology, Poland [1]
MSc, Structural Engineer, White Young Green Ireland Ltd., Limerick, Ireland [2]

1. Introduction

In historic timber structures in opposite to modern ones the all-timber connection have been commonly used (see
Figure 1) [1]. The structures have served us well over the centuries proving their durability. But now many of them are in need of repair.

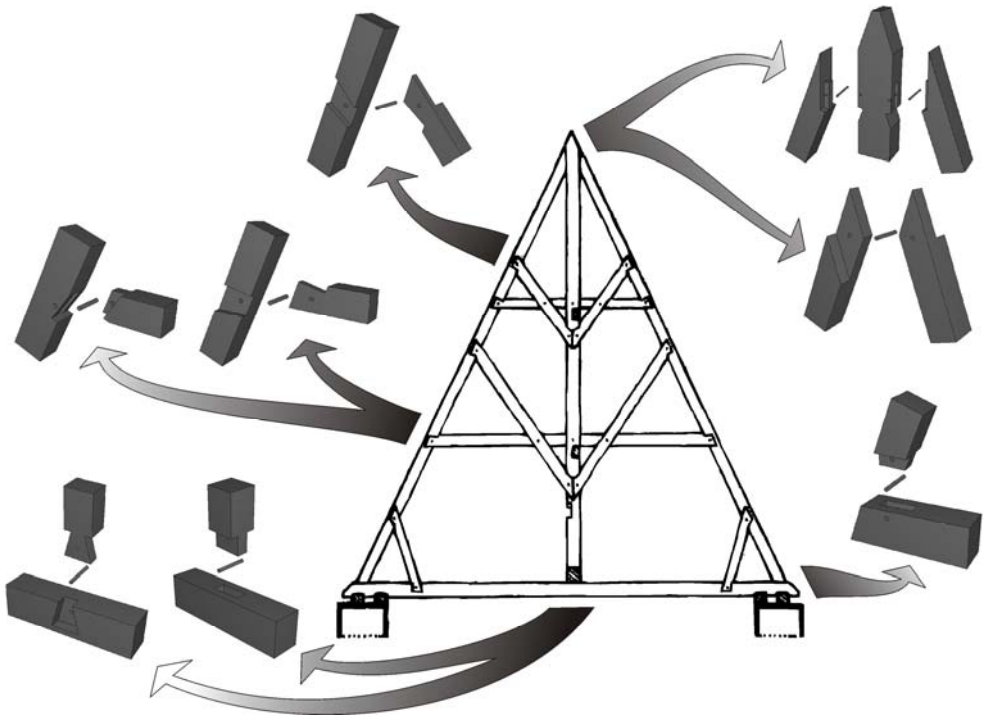

Figure 1. Joints in commonly used over the 15th to early 19th centuries around territory of Poland carpenter work structures of church roofs

Joints in carpenter work structures are usually the most loaded portions of them on one hand and the most subtle on the other hand, therefore the most exposed to failure following overloading as well as damage by dampness or vermin. The sizes of carpenter work structure members are usually increased comparing to the ones theoretically required to carry the loads and provide adequate stiffness in order to accommodate

joins. Hence the decrease in cross-section along member length does not usually threaten the overall strength and stability of structure so much as damage of element of joint, which causing the loss of stiffness and decreasing the ability to carry the loads by joints can easily lead to subsequent loss of strength or extensive deformation of structure.
Timber frame carpentry developed many centuries before rational engineering design and analysis [1], [2]. There is little rational basis for design of even the simplest joints or frames. In keeping with tradition, joints and frames are primarily proportioned by the craftsman through historic precedents. Modern timber engineering design codes of practice offer little or no assistance to the structural engineer making an attempt to assess strength and serviceability of joints. Proof loading of structures has become commonplace while rational engineering design fail to convince.
The knowledge and understanding of behaviour of joints seems to be critical to the ability of assessment of overall safety level of structure, which even with partially damaged elements can still remain to be capable to carry the loads. In connection to the desire to repair historic structures in a manner, which affects the historical fabric as little as possible such knowledge can consequently help a structural engineer to recognize the possible way of load distribution in undamaged members and the effective, feasible and in the same time least affecting the historic fabric way of repair or strengthening of the structure.
The paper is intended to present the overall approach to computational modeling of all-timber joints in carpenter work structure with account taken for complexity of material itself as well as the requirement of 3-dimentional modeling in order to avoid the simplifications required to assemble the model in plane stress system. The work follows the previous research [3], [4], [5], [6], [7], [8] and literature study as denoted in text.

2. Model development – wood anisotropy

In general case wood is an highly anisotropic material but usually it can be simplified to orthotropic one with three mutually perpendicular material directions *L, R* and *T* coinciding with respectively parallel to grain direction (*L*), and two transversal directions: radial (*R*) – perpendicular to growth rings and tangential (*T*) – parallel to growth rings.
The longitudinal modulus of elasticity is usually 10-20 times larger than radial or tangential modulus, while those transversal modules can differ by less then a factor of two. In addition to that the actual radial and tangential directions differ around the cross-section of element. It is then the rational proposal to replace the tangential and radial modules of elasticity with the E_{RT}, average for both mentioned directions.
However, it needs to be underlined here that it is not recommended to simplify material model to transversal isotropy. In an isotropic plane, the shear modulus is typically approximately equal to one-third of modulus of elasticity depending on Poison's ratio, but in wood transverse shear modulus G_{RT} is usually 10-20 times smaller than transversal modulus of elasticity [9].
The elastic constitutive equation in contracted notation is defined:

$$\sigma_i = D_{ij}\varepsilon_i \tag{1}$$

which expands for material of considered kind into [4], [10]:

$$\begin{Bmatrix}\sigma_1\\ \sigma_2\\ \sigma_3\\ \sigma_4\\ \sigma_5\\ \sigma_6\end{Bmatrix} = \begin{bmatrix} D_{11} & D_{12} & D_{12} & 0 & 0 & 0\\ & D_{22} & D_{23} & 0 & 0 & 0\\ & & D_{22} & 0 & 0 & 0\\ & & & D_{44} & 0 & 0\\ & sym. & & & D_{66} & 0\\ & & & & & D_{66}\end{bmatrix} \begin{Bmatrix}\varepsilon_1\\ \varepsilon_2\\ \varepsilon_3\\ \varepsilon_4\\ \varepsilon_5\\ \varepsilon_6\end{Bmatrix} \tag{2}$$

For 6 independent engineering material properties: $E_L, E_{\overline{RT}}$, $\nu_{L\overline{RT}}$, $\nu_{\overline{RT}}$, $G_{L\overline{RT}}$ and $G_{\overline{RT}}$ the components of elastic stiffness tensor D_{ij} equate to:

$$D_{11} = E_L\left(1-\nu_{\overline{RT}}{}^2\right)\Psi, \qquad D_{22} = E_{\overline{RT}}\left(1-\frac{E_{\overline{RT}}}{E_L}\nu_{L\overline{RT}}{}^2\right)\Psi, \qquad D_{12} = E_{\overline{RT}}\nu_{L\overline{RT}}\left(1+\nu_{\overline{RT}}\right)\Psi,$$
$$D_{23} = E_{\overline{RT}}\left(\nu_{\overline{RT}}+\frac{E_{\overline{RT}}}{E_L}\nu_{L\overline{RT}}{}^2\right)\Psi, \qquad D_{44} = G_{\overline{RT}}, \qquad D_{66} = G_{L\overline{RT}} \tag{3}$$

where:

$$\Psi = \frac{E_L}{E_L\left(1-\nu_{RT}^2\right)-2E_{\overline{RT}}\nu_{L\overline{RT}}{}^2\left(1+\nu_{\overline{RT}}\right)} \tag{4}$$

The stress-strain relations for uniaxial tests in parallel (*L*) and perpendicular to grain (*RT*) direction is shown in *Figure 2* and *Figure 3* respectively [11], [12], [13], [14], [15].

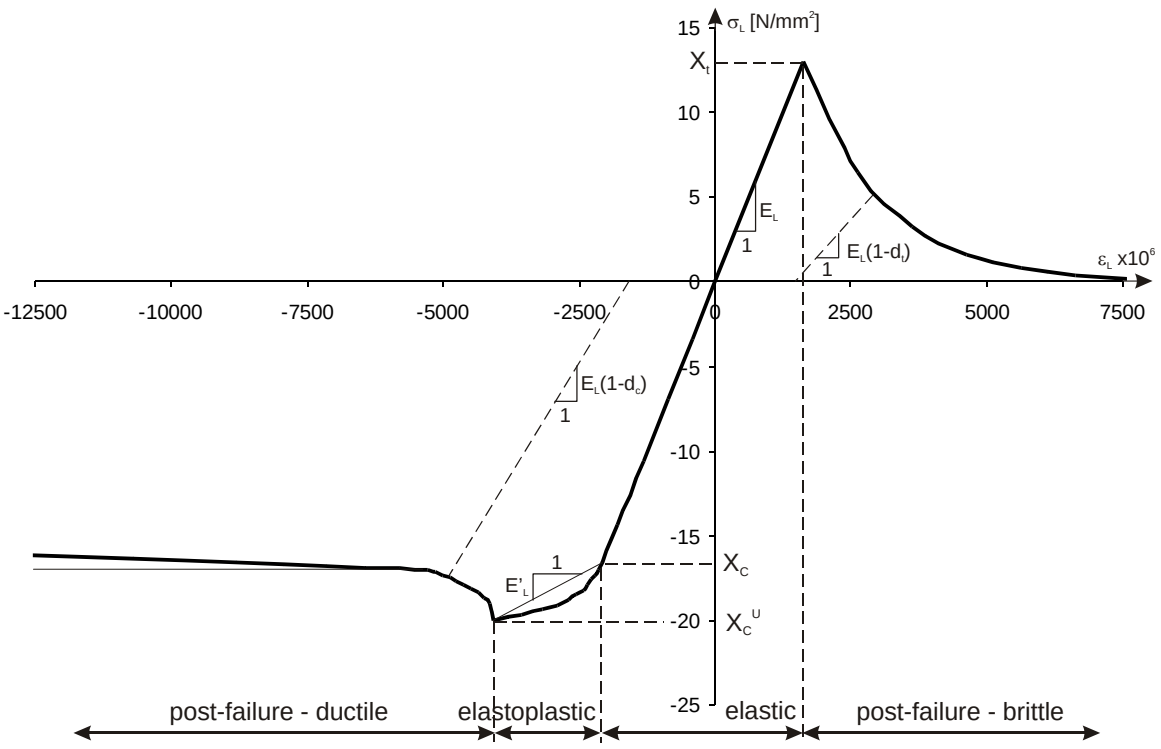

Figure 2. Stress-Strain relation for wood in uniaxial test in parallel to grain (L) direction. Idealized curve (thick line) and simplified one (thin line)

The model being developed in the study addresses the mechanical behaviour of real pine wood material of historic timber structure and is intended to make possible ultimate prediction of stress-strain relation in tri-axial stress state. The values of strength in parallel and perpendicular to grain direction depicted in figures, different for tension and compression, reflect the values for real material with discontinuities and correspond to the ones given by the adequate code of practice [16] for timber of lower grade.
Curves presenting stress-strain relationship are split into elastic, elastic-plastic and post-failure portions to indicate different material behaviour following different rates of strains.

Elastic-plastic behaviour with nonlinear hardening wood presents generally in compression and it cannot be neglected but can be simplified to linear with tangent Young's modulus *E'* applied in this portion. Such an approach gives a reasonably good consensus between requirement of good material behaviour prediction and simplification limiting time needed for finding a solution [11]. The material model does not take into account any nonlinearity in elastic-plastic relation for tension considering it as an insignificant.
Once the stress reaches the ultimate strength, which corresponds to yield strength in tension the curves enter the post-failure zone. For post-failure portions on both tension and compression sides the relation is assumed to be perfectly plastic. Subsequently the hardening in post-failure zone for compression perpendicular to grain is neglected. The softening behaviour corresponding to brittle failure is proposed to be modeled by stiffness degradation caused by reduction of effective cross-section area following the cracks development. On damage mechanics theory basis [17] the degradation variable *d* is introduced, which is equal to 0 for intact material, and 1 for completely damaged one. Intermediate values describe failure rate which corresponds to crack development level in material point. Generally in tension brittle failure occurs which leads to progressive material damage until complete loss of strength.
In compression material presents ductile mode of failure demonstrated in long plateau region leading to another hardening region where material recovers the initial stiffness [11], [12]. Such a behaviour is common for porous materials. This region, however, cannot be reach until extensive rate of deformation occurs hence is not considered in presented approach.
For compression parallel to grain, however, limited material degradation also is visible. The stress-strain curve declines initially to the level equating to approximately $0.85X_c^u$ [15].

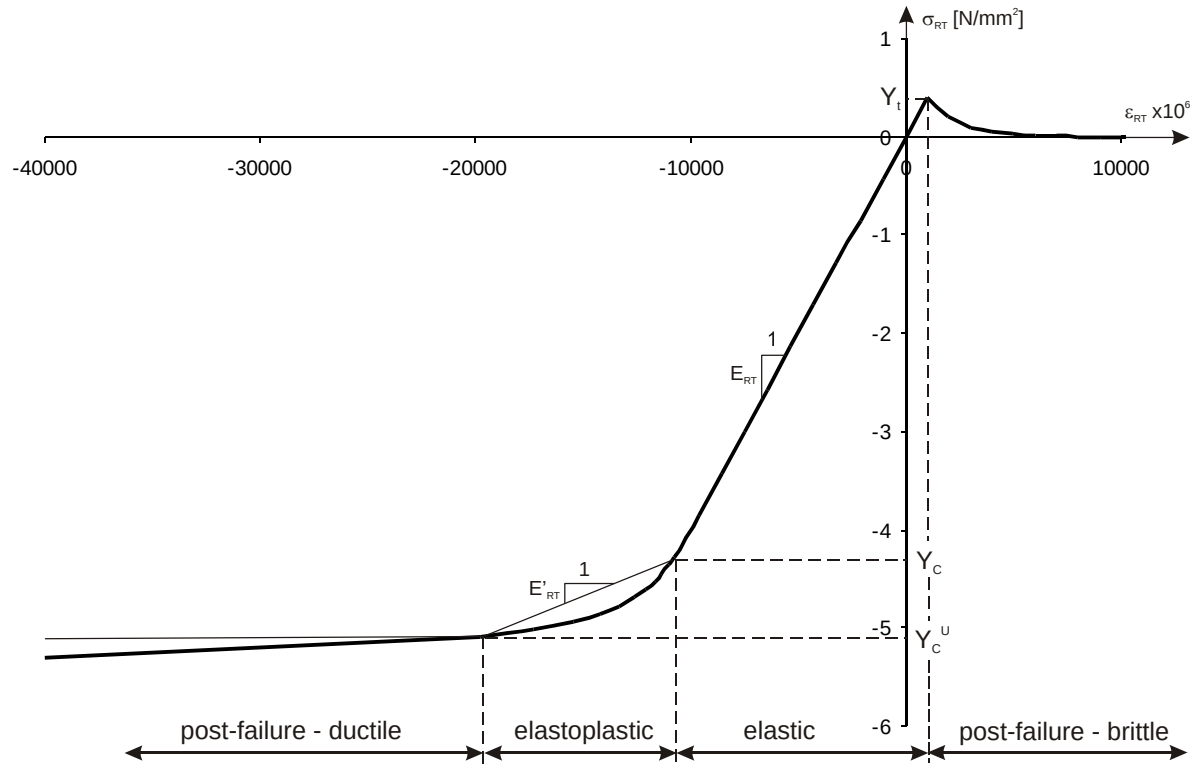

Figure 3. Stress-Strain relationship for wood in uni-axial test in perpendicular to grain (R and T) directions. Idealized curve (thick line) and simplified one (thin line)

The Failure in wood is also brittle for shear [15]. The material looses his strength after reaching the ultimate strength value. The mechanism is similar as for tension.
Below one can find set of material properties for pine wood for historic timber structures.

E_L	8000 MPa	G_{LRT}	570 MPa	X_c	17 MPa	Y_c^u	5.1 MPa
E'_L	1530 MPa	G_{RT}	57 MPa	X_c^u	20 MPa	Y_t	0.4 MPa
E_{RT}	400 MPa	v_{LRT}	0.39	X_t	13 MPa	S	2.4 MPa
E'_{RT}	90 MPa	v_{RT}	0.47	Y_c	4.3 MPa	Q	1.2 MPa

3. Hill's Yield Criterion

Proposed by Hill [18] yield criterion for orthotropic 3-diamentional body is described by equation:

$$2f(\sigma_k) \equiv F(\sigma_2-\sigma_3)^2 + G(\sigma_3-\sigma_1)^2 + H(\sigma_1-\sigma_2)^2 + 2L\sigma_4{}^2 + 2M\sigma_5{}^2 + 2N\sigma_6{}^2 = 1 \tag{5}$$

where coefficients equate to

$$\begin{aligned} &2F = \frac{1}{Y^2}+\frac{1}{Z^2}-\frac{1}{X^2}, \quad && 2G = \frac{1}{Z^2}+\frac{1}{X^2}-\frac{1}{Y^2}, \quad && 2H = \frac{1}{X^2}+\frac{1}{Y^2}-\frac{1}{Z^2}, \\ &2L = \frac{1}{Q^2}, && 2M = \frac{1}{R^2}, && 2N = \frac{1}{S^2} \end{aligned} \tag{6}$$

Assuming the material properties in axes perpendicular to grain are equal, we can state that $G=H$, $M=N$ and $S=T$. The coefficients simplify then to

$$2F = \frac{2}{Y^2}-\frac{1}{X^2}, \quad 2G = 2H = \frac{1}{X^2}, \quad 2L = \frac{1}{Q^2}, \quad 2M = 2N = \frac{1}{S^2} \tag{7}$$

4. FE analysis and photo-elasticity test results of chosen carpenter work connections

Below in Figure 4, Figure 5 and Figure 6 are presented the results of FE analysis of chosen types of all-timber connection of timber roof structure shown in Figure 1. The material model developed in [3] and also presented in [4] is basing on Hill's yield criterion. This yield criterion brings some certain limitations to model development which need to be taken into consideration before performing the analysis.

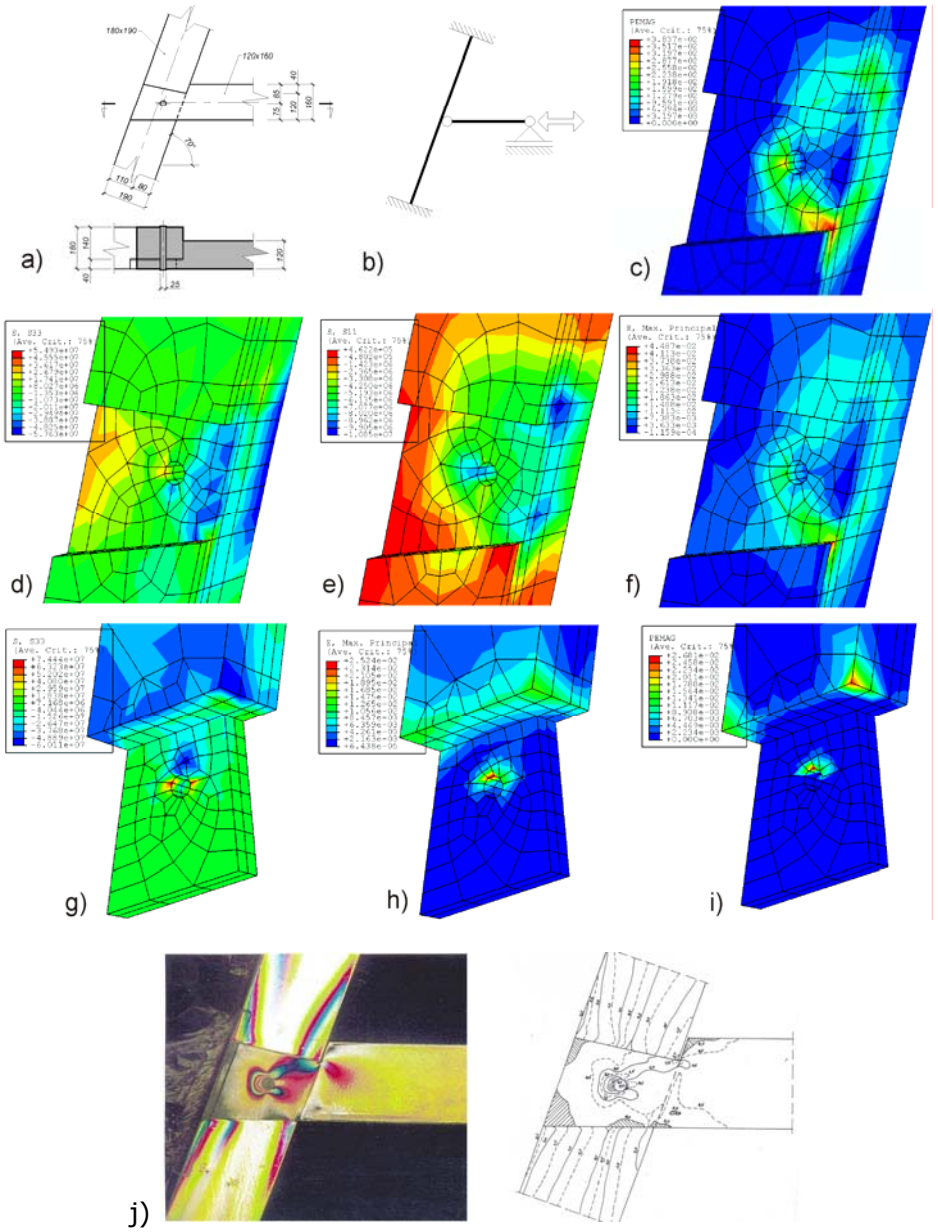

Figure 4. Collar beam to rafter connection analysis results [4]. (a) connection dimensions, (b) static scheme, (c) plastic strains in rafter, (d) stresses parallel to member centerline in rafter, (e) stresses perpendicular to member centerline in rafter in plane of connection, (f) total strains in rafter, (g) stresses parallel to member centerline in collar, (f) total strains in rafter, (g) stresses parallel to member centerline in collar, (h) total strains in collar beam, (i) plastic strains in collar beam, (j) photo-elasticity test

The introduced by Hill in 1950 [18] yield criterion for orthotropic material was developed from Mises criterion for isotropic material to provide the way of describing the phenomenal behaviour of steel, which in conditions when extensive plastic deformation occurs presents an orthotropic body properties.
The criterion does not take into account the different magnitudes of yield strengths in compression and tension in the same material axis direction. Also coupling between strengths in different directions is arbitrary and fixed.

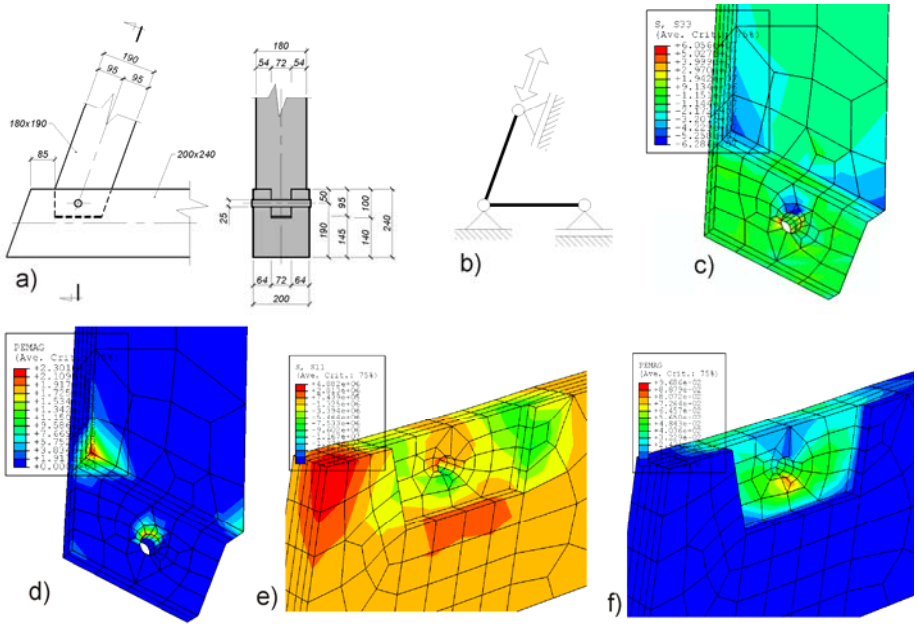

Figure 5. Rafter to stretcher connection analysis results [4]. (a) connection dimensions, (b) static scheme, (c) stresses parallel to member centerline in rafter, (d) plastic strains in rafter, (e) stresses perpendicular to member centerline in stretcher in member plane, (f) plastic strains in stretcher

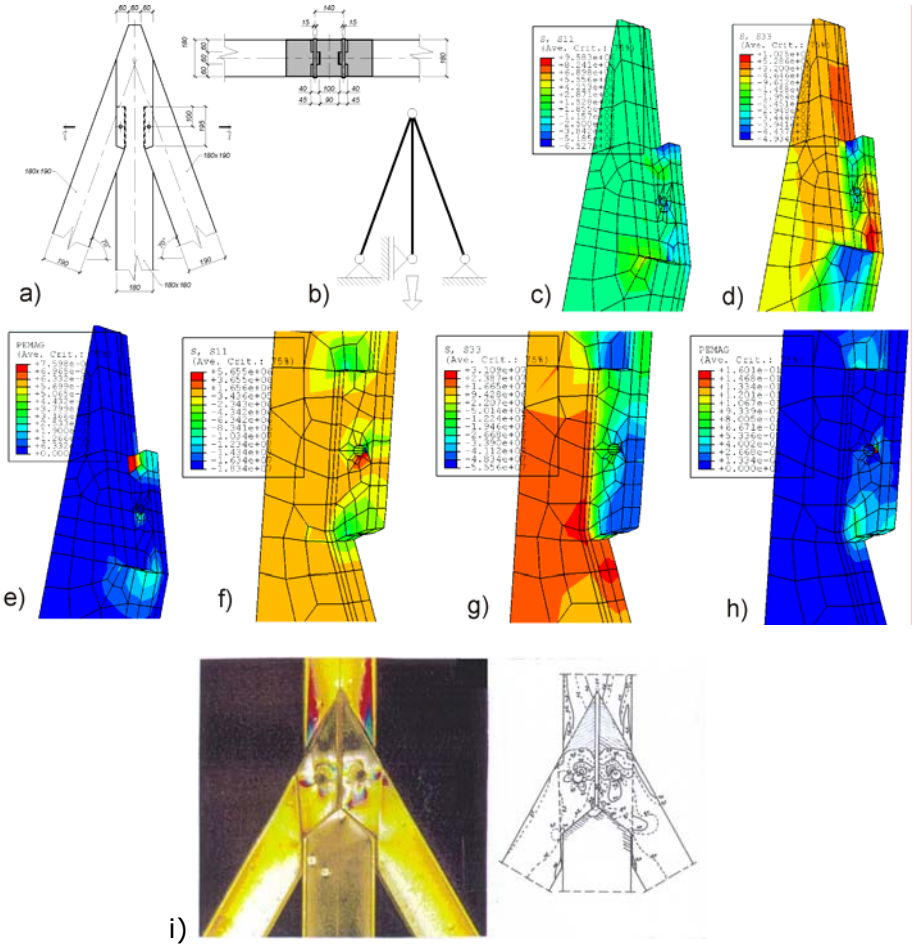

Figure 6. Rafter to hanger ridge connection analysis results [4]. (a) connection dimensions, (b) static scheme, (c) stresses perpendicular to member centerline in rafter in plane of connection, (d) stresses parallel to member centerline in rafter, (e) plastic strains in rafter, (f) stresses perpendicular to member centerline in hanger in plane of connection, (g) stresses parallel to member centerline in hanger, (h) plastic strains in hanger, (i) photo-elasticity test

For analysis, of which results are presented here the material with yield strengths equate to yield strength of wood in compression was arbitrary taken. The load cases considered generally cause the compression stresses. The tension appears only locally, usually in direction perpendicular to the applied force vector in stress concentration locations.
The results have shown that allowing for plastic deformation in connections can significantly increase the capacity of same, especially in pegged connections where plastic deformations occurs in relatively early state. Pegs, which are generally being bent cause that surface of opening is loaded pretty unequally, which subsequently leads to concentration of stresses there and appearing of local plastic deformations in quite early state.

However not taking into account the difference between tensile and compressive strengths magnitude can lead to the increase of the value of connection stiffness.

The test of joints using photo-elasticity method were made in Wroclaw University of Technology under supervision of dr L. Jankowski [5], [6].

5. Polynomial strength formula for wood

To avoid the disadvantages of using of Hill's criterion for prediction of structural timber members behaviour the tensor polynomial criterion for anisotropic materials proposed by Tsai and Wu [19] is proposed. The criterion is generally described by the following equation:

$$f(\sigma_k) \equiv F_i \sigma_i + F_{ij} \sigma_i \sigma_j = 1 \tag{8}$$

where second and forth order strength tensor, in contracted notation F_i and F_{ij}, respectively, are expanding into:

$$F_i = \begin{Bmatrix} F_1 \\ F_2 \\ F_3 \\ F_4 \\ F_5 \\ F_6 \end{Bmatrix}, \qquad F_{ij} = \begin{bmatrix} F_{11} & F_{12} & F_{13} & F_{14} & F_{15} & F_{16} \\ & F_{22} & F_{23} & F_{24} & F_{25} & F_{26} \\ & & F_{33} & F_{34} & F_{35} & F_{36} \\ & & & F_{44} & F_{45} & F_{46} \\ & sym. & & & F_{55} & F_{56} \\ & & & & & F_{66} \end{bmatrix} \tag{9}$$

The linear terms in σ_i takes into account the internal stresses, which can describe the difference between tensile and compressive strength and quadratic terms σ_{ij} define an ellipsoid in the 6-dimentional stress-space.
Several features are associated with proposed stress criterion.
It is a scalar equation and automatically invariant. Interactions among all stress component are independent material properties. Being invariant eq. (8) is valid in all coordination systems and since strength components are expressed in tensors we can readily transform them to another coordination system or equivalently rotate in the opposite direction the applied stresses.
Certain stability components are incorporated in the stress tensors. For a thermodynamic allowable criterion (positive finite strain energy) the values F_{ij} must be positive and the failure surface has to be closed. Thus the magnitudes of interaction terms are constrained by the inequality:

$$F_{ii} F_{jj} - F_{ij}^2 > 0 \tag{10}$$

For orthotropic materials the off-diagonal terms in eq. (9), which are F_4, F_5, F_6 vanish. The coupling between the normal and shear stresses (e.g. F_{16}) also vanishes if we assume that change in sign of shear stress does not change the failure stress. For the

same reason the shear strengths for orthotropic material are all uncoupled (i.e. $F_{45} = F_{46} = F_{56} = 0$).
Assuming, in addition, that in transversal plane properties are equal in both directions we can immediately say that all indices associated with plane 2-3 are identical:

$$F_2 = F_3, \quad F_{12} = F_{13}, \quad F_{22} = F_{33}, \quad F_{55} = F_{66} \tag{11}$$

For practical use of such criterion the relations between strength tensors components and engineering strengths need to be found. The uniaxial compressive and tensile strengths can be easily obtained from tests performed on specimens oriented along the adequate axes. We can then assume that σ_1 is the only non-zero stress component in eq. (8) :

$$F_1\sigma_1 + F_{11}\sigma_1^2 = 1 \tag{12}$$

Applying $\sigma_1 = X_t$ and $\sigma_1 = -X_c$ in equation (12) we get two equations as follows

$$F_{11}X_t^2 + F_1X_t = 1, \qquad F_{11}X_c^2 - F_1X_c = 1 \tag{13}$$

Solving equations (13) simultaneously, we obtain

$$F_{11} = \frac{1}{X_tX_c}, \qquad F_1 = \frac{1}{X_t} - \frac{1}{X_c} \tag{14}$$

By essentially the same reasoning for 2-axis by substituting σ_2 with Y_t and $-Y_c$ we obtain

$$F_{22} = \frac{1}{Y_tY_c}, \qquad F_2 = \frac{1}{Y_t} - \frac{1}{Y_c} \tag{15}$$

By imposing pure shear in 1-2-plane and in 2-3-plane sequentially we obtain the shear strength in plane parallel to grain and perpendicular to grain respectively

$$F_{66} = \frac{1}{S^2}, \quad F_{44} = \frac{1}{Q^2} \tag{16}$$

To obtain the off-diagonal components of strength tensor like F_{12} value it is needed to perform the biaxial tension and compression test or to use the 45-degree off-axis specimens in uniaxial test as also discussed in [19] and shown for wood by Fleishmann [14].

Another approach presents Liu [20] taking into consideration proposed for (n = 2) by Hankinson for in 1921 well known and being widely used empirical formula for the magnitude of compressive strength of wood in a direction inclined at an angle to the grain as well as subsequently reported by other authors as being suitable also for tension (for value of n between 1.5 and 2):

$$\sigma_\theta = \frac{-X_cY_c}{X_c\sin^2\theta + Y_c\cos^2\theta}, \quad \sigma_\theta = \frac{X_tY_t}{X_t\sin^n\theta + Y_t\cos^n\theta} \tag{17}$$

Expressing the eq. (8) with respect to the *1'-2'* coordinate system at θ angle to *1-2* and assuming the only non-zero stress component is σ_θ we obtain

$$F'_1\,\sigma_\theta + F'_{11}\,\sigma_\theta^2 = 1 \tag{18}$$

Using then transformation relations of strength tensors shown in [19] and stress coefficients shown above in equations (14), (15) and (16) , equation (18) becomes

$$\left[\left(\frac{1}{X_t}-\frac{1}{X_c}\right)\cos^2\theta+\left(\frac{1}{Y_t}-\frac{1}{Y_c}\right)\sin^2\theta\right]\sigma_\theta+\left[\frac{\cos^4\theta}{X_tX_c}+\frac{\sin^4\theta}{Y_tY_c}+\left(2F_{12}+\frac{1}{S^2}\right)\sin^2\theta\,\cos^2\theta\right]\sigma_\theta^2=1 \quad (19)$$

Also equations (17) for n = 2 can be grouped as follows

$$\left(\sigma_\theta+\frac{X_cY_c}{X_c\sin^2\theta+Y_c\cos^2\theta}\right)\left(\sigma_\theta-\frac{X_tY_t}{X_t\sin^2\theta+Y_t\cos^2\theta}\right)=0 \quad (20)$$

Liu [20] shows by comparing equations (19) and (20) that the two equations are identical if

$$F_{12}=\frac{1}{2}\left(\frac{1}{X_tY_c}+\frac{1}{X_cY_t}-\frac{1}{S^2}\right) \quad (21)$$

Van der Put [21] confirms the correctness of eq. (21) for n = 2 deriving it in a different way by transforming the stresses rather then strength tensors and comparing with test results.
For plane transversal to grain Van der Put [21] shows that F_{23} for wood is relatively small, of much lower order than other components hence can be neglected. Also shows, that the F_{66} can be taken equal to $2F_{22}$, which can be used for lack of experimentally obtained value of shear strength in plane perpendicular to grain Q.

To Summarize the above we can now show the strength tensors from eq. (9) for wood as follows:

$$F_i=\begin{Bmatrix}\frac{1}{X_t}-\frac{1}{X_c}\\ \frac{1}{Y_t}-\frac{1}{Y_c}\\ \frac{1}{Y_t}-\frac{1}{Y_c}\\ 0\\ 0\\ 0\end{Bmatrix},\quad F_{ij}=\begin{bmatrix}\frac{1}{X_tX_c} & \frac{1}{2}\left(\frac{1}{X_tY_c}+\frac{1}{X_cY_t}-\frac{1}{S^2}\right) & \frac{1}{2}\left(\frac{1}{X_tY_c}+\frac{1}{X_cY_t}-\frac{1}{S^2}\right) & 0 & 0 & 0\\ & \frac{1}{Y_tY_c} & 0 & 0 & 0 & 0\\ & & \frac{1}{Y_tY_c} & 0 & 0 & 0\\ & & & \frac{1}{Q^2} & 0 & 0\\ & sym. & & & \frac{1}{S^2} & 0\\ & & & & & \frac{1}{S^2}\end{bmatrix} \quad (22)$$

6. Orthotropic plasticity formulation

Quadratic yield criterion for orthotropic material is written in general form [10], [22] as

$$f\equiv{\sigma_{eq}}^2(\sigma_i-\alpha_i,M_{ij})-k^2=0 \quad (23)$$

where σ_{eq} is effective stress or equivalent stress and k is threshold stress which is equal to the size of the yield surface. The Tsai-Wu criterion in form described previously by equation (8) is adapted to this general form in a way that the square of the effective stress is conveniently defined as

$${\sigma_{eq}}^2=M_{ij}(\sigma_i-\alpha_i)(\sigma_j-\alpha_j) \quad (24)$$

where the terms M_{ij} and $\alpha_i = \{\alpha_1, \alpha_2, \alpha_3, 0, 0, 0\}$ describe the shape of the yield surface and the surface origin defined as shifting stress, respectively, so that:

$$f \equiv M_{ij}(\sigma_i - \alpha_i)(\sigma_j - \alpha_j) - k^2 = 0 \tag{25}$$

expanding this one obtains

$$f \equiv M_{ij}\sigma_i\sigma_j - L_i\sigma_i - K = 0 \tag{26}$$

where

$$L_i = 2M_{ij}\alpha_j, \qquad K = -M_{ij}\alpha_i\alpha_j + k^2 \tag{27}$$

Comparing equations (27) and (8) it can be concluded that

$$M_{ij} = KF_{ij}, \qquad L_i = -KF_i \tag{28}$$

It can be seen that components of M_{ij} are not independent. Equating M_{11} to equality one can obtain $K=1/F_{11}=X_tX_c$ and $M_{12}=F_{12}/F_{11}$ etc.
Components α_i can be found by solving the following equations simultaneously

$$L_i = -KF_i = 2M_{ij}\alpha_j = 2KF_{ij}\alpha_j; \;\; i.e. \quad F_i = -2F_{ij}\alpha_j \tag{29}$$

which expands into

$$\begin{aligned} F_1 &= -2F_{11}\alpha_1 - 2F_{12}\alpha_2 - 2F_{12}\alpha_3 \\ F_2 &= -2F_{12}\alpha_1 - 2F_{22}\alpha_2 \\ F_3 &= -2F_{12}\alpha_1 - 2F_{22}\alpha_3 \end{aligned} \tag{30}$$

And as a result one obtains

$$\alpha_1 = \frac{F_1F_{22} - 2F_2F_{12}}{4F_{12}{}^2 - 2F_{11}F_{22}}, \qquad \alpha_2 = \alpha_3 = \frac{F_2F_{11} - F_1F_{12}}{4F_{12}{}^2 - 2F_{11}F_{22}} \tag{31}$$

And finally, the square of threshold stress can be calculated from eq. (27) with eq. (31) taken into account

$$k^2 = \frac{1}{F_{11}}(1 + F_{11}\alpha_1{}^2 + 4F_{12}\alpha_1\alpha_2 + 2F_{22}\alpha_2{}^2) \tag{32}$$

7. Subsequent yield surfaces

Subsequent yield surfaces are described with function

$$f \equiv \sigma_{eq}{}^2(\sigma_i - \alpha_i, M_{ij}(\varepsilon_{eq}^p)) - k^2(\varepsilon_{eq}^p) = 0 \tag{33}$$

where now, M_{ij} and k are functions of effective plastic strain $\varepsilon_{eq}{}^p$ acting as hardening parameter derived by equating the work done during plastic deformation in an uniaxial test to that produced by the effective stress and effective plastic strains.

Figure 7 and Figure 8 show the sections of initial and subsequent yield surfaces along the plane parallel to grain and perpendicular to grain, respectively.

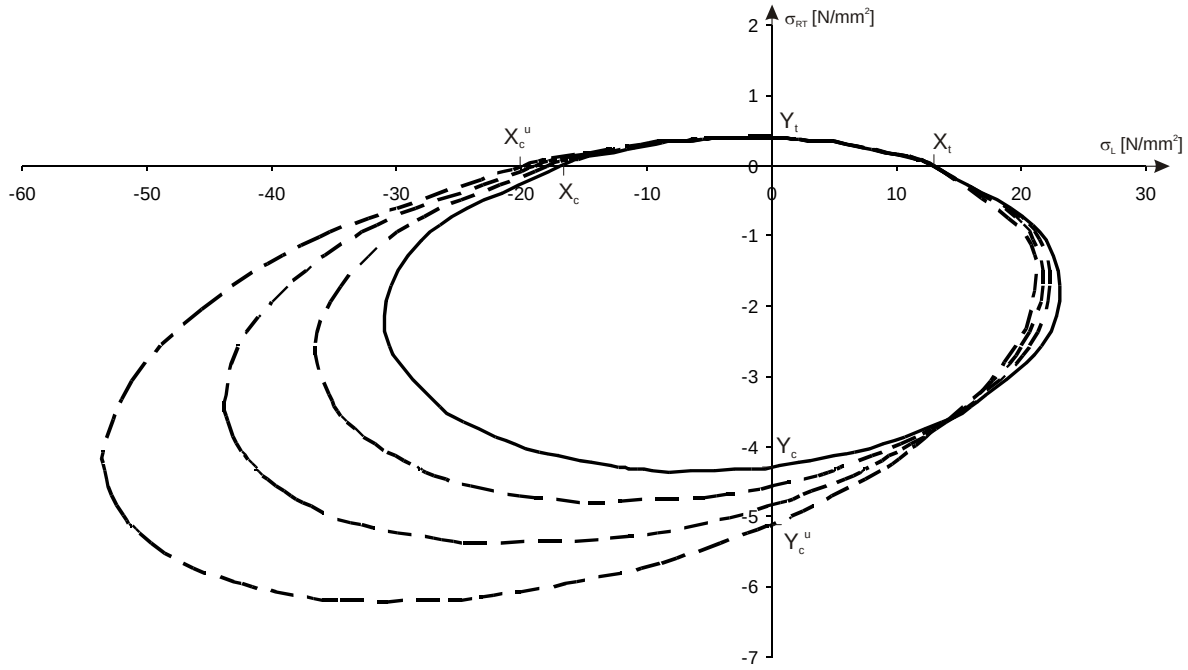

Figure 7. Section in 1-2-plane parallel to grain of initial (continues line) and subsequent yield surfaces (dashed lines)

In deriving the relationship between k and ε_{eq}^{p}, one-to-one relationship was assumed

$$k = k_0 + H'\varepsilon_{eq}^{p} \tag{34}$$

where *H′* can be found from uniaxial test for *E* – elastic modulus and *E′* – tangential modulus of elasto-plastic portion of stress-strain curve, through the formula:

$$H' = \frac{E'}{1 - \frac{E'}{E}} \tag{35}$$

Strength tensor M_{ij} components also vary with plastic deformation. The updated after detection of yielding strength parameters X_c and Y_c calculated under the same assumption as for k value by Vaziri et al. in [23] are found to be:

$$X_c^2 = \frac{E_{p1}}{H'}(k^2 - k_0^2) + X_{c0}^2, \qquad Y_c^2 = \frac{E_{p2}}{H'}(k^2 - k_0^2) + Y_{c0}^2 \tag{36}$$

where subscript '0' refers to initial yield value and E_{p1} and E_{p2} are hardening parameters for uniaxial stress/strain curves for compression in parallel to grain and perpendicular to grain direction respectively, which value are found to be as follows (with subscript 'u' referring to ultimate value):

$$E_{p1} = H'\frac{X_{cu}^2 - X_{c0}^2}{\left[1 + (X_{cu} - X_{c0})\right](X_{cu} - X_{c0})}, \qquad E_{p2} = H'\frac{Y_{cu}^2 - Y_{c0}^2}{\left[1 + (X_{cu} - X_{c0})\right](X_{cu} - X_{c0})} \tag{37}$$

Although shifting stress tensor α_i components are not independent parameters of subsequent yield surface their values also vary when plastic strain increase. Their updated values can be derived from equations (31) by substitution of updated values of strength parameters from eq. (36) into eq. (22).

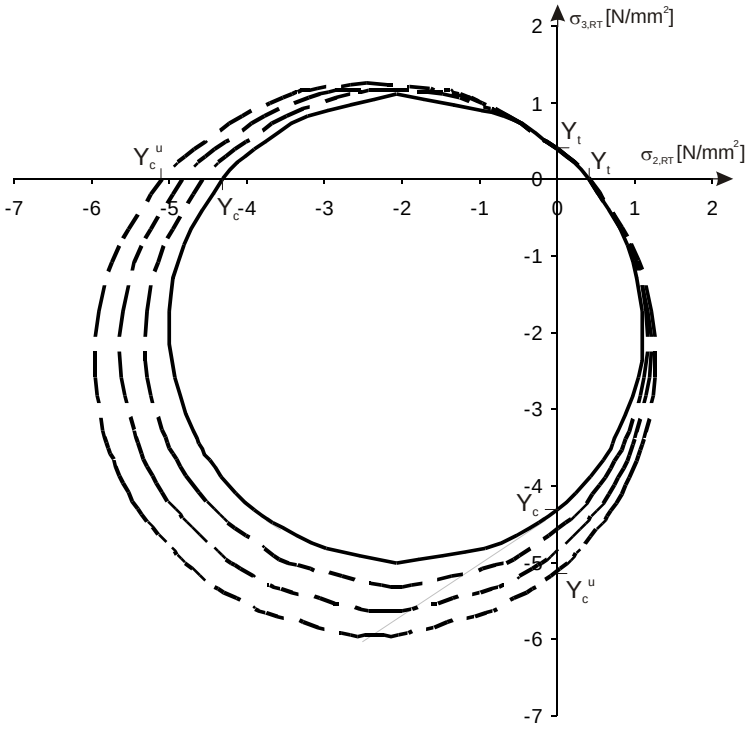

Figure 8. Section at 2-3-plane perpendicular to grain of initial (continues line) and subsequent yield surfaces(dashed lines)

The strain in elastic-plastic zone can be decomposed into elastic and plastic components, which in incremental form can be expressed as:

$$d\varepsilon_i = d\varepsilon_i^{el} + d\varepsilon_i^{pl} \tag{38}$$

And the associated with yield surface (23) plastic flow law:

$$d\varepsilon_i^{pl} = d\lambda \cdot \frac{\partial f}{\partial \sigma_i} \tag{39}$$

The constitutive equation then can be shown, as:

$$d\sigma_i = D_{ij}\left(d\varepsilon_i - d\lambda \cdot \frac{\partial f}{\partial \sigma_i} \right) \tag{40}$$

Provided that loading conditions are satisfied, the plastic hardening occurs. Equation (40) can be expressed as **Errore. L'origine riferimento non è stata trovata.**:

$$d\sigma_i = D_{ij}^{ep} d\varepsilon_i \tag{41}$$

where D_i^{ep} is the elastoplastic material stiffness tensor.
For unloading and neutral processes the constitutive rule from eq.(1) in incremental form is valid

$$d\sigma_i = D_{ij} d\varepsilon_i \tag{42}$$

8. Post-failure behaviour of wood

Once the stress exceeds the ultimate stress value (See *Figure 2* and *Figure 3*) material enters the post-failure zone. While in tension the damage mechanism becomes activated. The scalar damage variable *d* is introduced, which represent the ratio of hypothetic cracks area to the whole area of cross section. The value of damage variable is between

0 for undamaged material to *1* for completely destroyed.
The damage is defined in terms of effective stress $\tilde{\sigma}_i$ [17], which represents stress in undamaged portion of material cross-section and is generalized through relation:

$$\sigma_i = (1-d)\tilde{\sigma}_i = (1-d)D_{ij}\left(\varepsilon_i - \varepsilon_i^{pl}\right) \tag{43}$$

where:

$$(1-d) = (1-d_t)(1-d_c) \tag{44}$$

To account for different damage mechanism for tension and compression, damage state is described by two independent variable, d_c and d_t for compression and tension, respectively. The unloading stress-strain relation for partially damaged material is shown in *Figure 2*.
As failure/yield polynomial criterion introduced in equation (8) does not distinguish the mode of material failure, it is essential to define conditions of tension and compression dominance of stress-state in material point. Clouston et al. in [11] define the conditions for plane stress system which expand into 6-dimentional model. The distinction is made depending on the combination of stresses at the point of failure.
Let's define first the scalar variables reflecting the magnitude of individual stress components as:

$$\rho_i = M_{ii}\left(\sigma_i^2 - 2\sigma_i\alpha_i + \alpha_i^2\right), \quad \text{for } i=1,2,3 \quad \text{and} \quad \rho_i = M_{ii}\sigma_i^2, \quad \text{for } i=4,5,6 \tag{45}$$

The condition for tension dominance and thereby brittle failure are then:

$$\begin{aligned}
&(1)\ \sigma_1 \geq X_t, \quad (2)\ \sigma_2 \geq Y_t, \quad (3)\ \sigma_3 \geq Y_t, \quad (4)\ |\sigma_4| \geq Q, \quad (5)\ |\sigma_5| \geq S, \quad (6)\ |\sigma_6| \geq S,\\
&(7)\ \sigma_1 \geq 0 \ \textit{and}\ \rho_1 \geq \rho_2 \ \textit{and}\ \rho_1 \geq \rho_3, \quad (8)\ \sigma_2 \geq 0 \ \textit{and}\ \rho_2 \geq \rho_1 \ \textit{and}\ \rho_2 \geq \rho_3,\\
&(9)\ \sigma_3 \geq 0 \ \textit{and}\ \rho_3 \geq \rho_1 \ \textit{and}\ \rho_3 \geq \rho_2, \quad (10)\ \sigma_4 \geq \sigma_1 \ \textit{and}\ \sigma_4 \geq \sigma_2 \ \textit{and}\ \sigma_4 \geq \sigma_3,\\
&(11)\ \sigma_5 \geq \sigma_1 \ \textit{and}\ \sigma_5 \geq \sigma_2 \ \textit{and}\ \sigma_5 \geq \sigma_3, \quad (12)\ \sigma_6 \geq \sigma_1 \ \textit{and}\ \sigma_6 \geq \sigma_2 \ \textit{and}\ \sigma_6 \geq \sigma_3
\end{aligned} \tag{46}$$

All other cases of failure are than considered as ductile.

9. Conclusion

The Hill yield criterion for orthotropic material can only be used for wood under certain assumptions discussed in section 4. The criterion also comprises the assumption that material cannot fail under hydrostatic pressure, which is valid for most of structurally important materials but not necessarily for wood.
In spite of these disadvantages the presented results of analysis using this criterion in material model of joints show, that taking the non-elastic behaviour of wood into account during analysis can really show the relations in joints and help to develop the rules for assessing the capacity and safety level provided by all-timber connections in historic timber structures.
The comprehensive material model has than been proposed in paper reflecting the real mechanical behaviour of wood in timber structures. The model which includes the polynomial yield criterion capable to take onto account the difference between compressive and tensile strength magnitude and describes precisely the post-yielding and post-failure relationship removes all lacks existing in the model used so far.
The next step is to implement this model into Finite Element Analysis software package, which the work has already been commenced on.

Bibliographical references

[1] GANOWICZ R., 2000, *Historyczne więźby dachowe polskich kościołów*. Poznań, Poland. Wydawnictwo Akademii Rolniczej im. Augusta Cieszkowskiego w Poznaniu,.
[2] TAJCHMAN J., 2005, Propozycja systematyki i uporządkowania terminologii ciesielskich konstrukcji dachowych występujących na terenie Polski od XIV do XXw. Monument, nr 2/2005, str. 7-36, Warszawa.
[3] KARDYSZ M., 2006, *Analiza pracy statycznej połączeń stosowanych w drewnianych konstrukcjach zabytkowych.* Wrocław University of Technology – Faculty of Civil Engineering, Wroclaw, Poland. MSc Thesis.
[4] JASIEŃKO J., KARDYSZ M., 2006, *Analiza pracy statycznej połączeń stosowanych w drewnianych konstrukcjach zabytkowych (eng. Static behaviour of joints in historic timber structures).* Problemy remontowe w budownictwie ogólnym i obiektach zabytkowych (eng. Renovation problems in constructions and historic buildings), pp. 218-230, Wrocław, Poland. Dolnośląskie Wydawnictwo Edukacyjne.
[5] ENGEL L., 2006, *Wpływ formy konstrukcji na stan zachowania obiektów zabytkowych.* Wroclaw University of Technology – Faculty of Architecture, Wroclaw, Poland. PhD Thesis.
[6] ENGEL L., JANKOWSKI L., JASIEŃKO J., 18/2005, *Praca statyczna wybranych połączeń realizowanych w drewnianych konstrukcjach zabytkowych.* Wiadomosci Konserwatorskie.
[7] JASIEŃKO J., ENGEL L., GOSPODAREK T., 2005, *Elastooptische und numerische untersuchungen der ausgewaehlter verbindungen an hoelzerner denkmalkonstruktionen.* ANTIKON, Wismar, Germany.
[8] JASIEŃKO J., ENGEL L., RAPP P., 2006, *Study of strains and stresses in historical carpentry joints*. Proceedings of Sc. Conf.: Structural Analysis of Historical Constructions, New Delhi.
[9] NAIRN J. A.: *A Numerical Study of Transverse Modulus of Wood as a Function of Grain Orintation and Properties.* Holzforschung, in press, submitted 2007.
[10] BODIG J., JAYNE B.A., 1982, *Mechanics of Wood and Wood Composites*. New York, USA, Van Nostrand Reinhold Company.
[11] CLOUSTON P.L., LAM F.,2001, *Computational Modeling of Strand-Based Wood Composites.* Journal of Engineering Mechanics, Vol. 127, pp. 844-851, nr 8.
[12] HOLMBERG S., PERSSON K., PETERSSON H., 1999, *Nonlinear mechanical behaviour and analysis of wood and fibre materials.* Computer and Structures, Vol. 72, pp. 459-480.
[13] GROSSE M., RAUTENSTRAUCH K., SCHLEGEL R., 2005, *Numerische Modellierung von Holz und Verbindungselementen in Holz-Beton-Verbundkonstruktionen.* Bautechnik, Vol. 82, pp. 355-364, nr 6.
[14] FLEISCHMANN M., 2005, *Numerische Berechnung von Holzkonstruktionen unter Verwendung eines realitaetsnahen ortotropen elasto-plastischen Werkstoffmodells.* Vienna, Austria. PhD Thesis.
[15] POULSEN J. S., *Compression In Clear Wood,* 1998*,* Technical University of Denmark, Department of Structural Engineering and Materials. Lyngby, Denmark. PhD Thesis,
[16] PN-B-03150:2000, *Konstrukcje drewniane. Obliczenia statyczne i projektowanie.*
[17] SKRZYPEK J., *Podstawy Mechaniki Uszkodzeń*, 2006, Krakow, Poland, Wydawnictwo Politechniki Krakowskiej
[18] HILL R., 1950, *The Mathematical Theory of Plasticity*. Oxford, UK. The Clarendon Press.
[19] TSAI S. W., WU E. W., 1971, *A General Theory of Strength for Anisotropic Materials.* Journal of Composite Materials, Vol. 5, pp. 58-80.
[20] LIU J. Y., 1984, *Evaluation of the Polyniomial Strength Theory for Woods.* Journal of Composite Materials, Vol. 18, pp. 216-226.

[21] VAN DER PUT T.A.C.M., 2005,*The Tensorpolynomial Failure Criterion for Wood.* Delft Wood Foundation Publication Series 2005, nr 2.
[22] GABRYSZEWSKI Z., 2001, *Teoria sprężystości i plastyczności*. Wroclaw, Poland. Oficyna Wydawnicza Politechniki Wrocławskiej.
[23] VAZIRI R., OLSON M. D., ANDERSON D. L. ,1991, *A plasticity-based constitutive model for fibre-reinforced composite laminates.* Journal of Composite Materials, Vol. 25, pp. 512-535, nr 5.
[24] JIRASEK M., BAZANT Z. P., *Inelastic Analysis of Structures*. Chichester, UK. John Willey & Son